J. Quant. Spectrosc. Radiat. Transfer Vol. 42, No. 3, pp. 247–251, 1989
Printed in Great Britain.

0022-4073/89 $3.00 + 0.00

PRECISE MEASUREMENT OF THE BALMER-ALPHA CORE

MANUEL A. GONZÁLEZ, VÍCTOR R. GONZÁLEZ, and SANTIAGO MAR
Departamento de Física Aplicada III, Facultad de Ciencias, Universidad de Valladolid, Valladolid 47071, Spain

(*Received* 6 *June* 1988; *received for publication* 3 *February* 1989)

Abstract—We have obtained a precise spectrum of the Balmer-alpha line, corrected for self-absorption effects, from a constant-electron-density plasma with different optical depths, in order to compare it with theoretical models and simulation techniques. The reconstruction process of the non-self-absorbed profile is highly reproducible and may be applied to both optically-thin and thick plasmas.

INTRODUCTION

The authors of recent calculations,[1,2] based on computer simulation, have utilized the VCS (Vidal et al[3]) and KG (Kepple and Griem[4]) theories. The purpose was to test their validity, as well as to measure ion-dynamic effects proposed by Wiese.[5] These effects are especially strong in the central regions of the Lyman and Balmer spectral lines. Several workers[6–10] have published experimental data that may be compared with theoretical calculations. However, most of these refer to the Lyman-alpha and Balmer-beta lines. For this reason, it is desirable to make measurements near the centre of the Balmer-alpha line. This line profile exhibits strong self-absorption. In a previous study,[11] a simple procedure was proposed to control this effect in the line wings. The procedure may be extended to the line core. Self-absorption is controlled by performing measurements on plasmas at constant electron density and for different optical depths. Next, we reconstruct a non-self-absorbed profile, as will be explained. All of the reconstructed profiles must be the same, except for experimental errors.

EXPERIMENTAL STUDIES

The plasma source was formed in a 150-mm long Pyrex cylinder, with an i.d. of 18.2 mm. Two annular pieces of aluminium were glued to the ends and served as electrodes. To avoid cathode effects, the plasma chamber was screened from the electrodes. The electrical wires were attached symmetrically to the electrodes in order to preserve plasma symmetry. The discharge tube was filled with argon containing 2–9.6% hydrogen. The plasma was produced by a 9.20 ± 0.01 kV electrical discharge between the two electrodes. We have verified that the influence of the lamp windows on the plasma is not important. Our axial measurements correspond to a homogeneous plasma zone that is located around the central axis of the source; axial isolation was accomplished with two 3-mm dia diaphragms separated by 90 cm. The spatial resolution was 1/300 rad.

The experimental set-up consisted of an optical multichannel analyser, which activated the excitation unit in which the electrical discharge took place, and of a Jobin–Ivon monochromator with two 1500-mm focal length spherical mirrors working in the first order. The grating had 1200 lines/mm. The photomultiplier allowed us to record the light pulse, which was amplified and then applied to the input of the polarization circuit of a vidicon, thereby allowing us to avoid some randomness at the instant of lamp ignition. The polarization pulse-generator of the vidicon controls the instant at which the spectrum is recorded, as well as the width of the polarization pulse in the electrostatic lens of the detector. The vidicon has 500 channels, each of which is 25 μm wide, which is equivalent to 0.13 Å for the Balmer-alpha line. With our instrumental resolution, profile distortion was negligible. The signal registered on the vidicon is transferred to the OMA, which yields a digital output of the spectrum.

Self-absorption was measured by means of a lens and a flat mirror imaging the lamp centre on itself. The images of other points of the lamp were in symmetrical positions with respect to the centre. In this manner, the emergent light through the back of the lamp was reflected and reintroduced into the dischange tube.

The optical depth is

$$\tau(\lambda) = \ln\{(A-1)/[B(\lambda)-1]\}, \tag{1}$$

where A is the ratio of the signals with and without the reflected light included, as measured at an optically-thin wavelength (e.g., in the line wings), while $B(\lambda)$ is the ratio at the wavelength λ. This expression is exact for the case in which the temperature is uniform along the line of sight, even if the absorption coefficient varies because of concentration changes.[5]

Standard techniques were used for alignment and calibration. Different optical depths were obtained by varying the pressure inside the plasma chamber, which was controlled with a precision of 0.1 mbar. The H_2 and Ar flows were controlled with a precision of 0.01 and 1 cm^3/min, respectively. Measurements were taken in the final decay zone of the plasma. By choosing the instant of measurements properly, all of the electron densities were the same for every test. The 430.0 nm line of ArI was used as a monitor[11,12] in order to maintain identical electron densities ($\sim 1 \times 10^{17}$ cm^{-3}). In order to reduce vidicon errors, we proceeded as follows. The measurements corresponding to each discharge were individually transferred to the computer. Two measurements were taken while avoiding light entry into the monochromator, after each set of 10 discharges. After 40 discharges, we performed measurements with an irradiance lamp with a uniform spectrum in order to estimate the system response. For data processing, our procedure provided information on and allowed removal of vidicon noise; facilitated measurements of small differences in the vidicon channels in order to improve the data; and gave information on the reproducibility of the measurements.

The final errors were estimated to be $<2\%$.

RESULTS AND DISCUSSIONS

In Table 1, we list five sets of experimental conditions that give rise to five different self-absorbed profiles. The optical depth of each was computed from Eq. (1). Each observed profile represents an average of 10 scans, with each scan yielding approx. 450 points. From each observed profile, we reconstructed the respective corrected Balmer-alpha profile without self-absorption by using the equation

$$I'(\lambda) = I(\lambda) \times \tau(\lambda)/\{1 - \exp[-\tau(\lambda)]\} \tag{2}$$

where $I(\lambda)$ is the observed profile without reflected light and $I'(\lambda)$ is the corrected profile. It can be seen from Table 2 that the full half-width and the intensity at the central wavelength for each corrected profile are practically the same. The differences in half-widths are $<2\%$ and those of the central intensities are $<2.5\%$, in spite of different initial self-absorption conditions. The observed profiles in experiments 1, 3 and 4 are shown in Fig. 1; the results of experiments 2 and 5 fall

Table 1. Experimental conditions for the observed Balmer-alpha profiles.

Experiment number	1	2	3	4	5
Pressure, mbar	12.3	12.3	12.2	11.7	11.7
Flow rates, Ar	19.70	18.29	19.70	23.92	19.70
cm^3/min H_2	0.41	0.91	0.90	0.91	1.90
Measurement time, μs	30	30	30	35	35
Optical depth at the peak	0.311	0.426	0.493	1.123	1.156

Table 2. Characteristics of the corrected profiles.

Experiment number	1	2	3	4	5
Full half-width, Å	11.63	11.22	11.32	11.49	11.57
Intensity of the line peak, $(Å)^{-1}$	0.0609	0.0632	0.0624	0.0614	0.0631

practically on top of those for the third and fourth experiments and have been omitted for brevity. In Fig. 1, we also show the averaged corrected profiles with error bands, which were calculated by overestimating the standard sample deviation. The area under the curve of the corrected profile has been normalized to unity; it was calculated after removing the parasite line that appears in the blue wing. It may be inferred from Table 2 that the Balmer-alpha line without self-absorption has a full half-width of $\Delta\lambda_{1/2} = (11.45 \pm 0.21)$ Å and an intensity at the central wavelength of the profile equal to (0.0622 ± 0.0013) $(Å)^{-1}$ for our experimental conditions.

The reconstruction process introduces an error smaller than 3.5% between the centre and the wings of the profile. However, the method becomes especially noisy in the wings of the profile, since $B(\lambda)$ and hence $\tau(\lambda)$ [see Eq. (1)] have sizeable fluctuations in these regions because the magnitudes of the measurements are comparable with their deviation. Thus, beyond 9 Å from the line centre, the reconstruction error increases gradually and reaches 10% in the wings. We also note some increase in the reconstruction error around the line centre. This increase occurs even though $B(\lambda)$ and $\tau(\lambda)$ have small variations in this region, because their values are small; as a result, the relative errors increase to 4.5%.

The reconstructions (see Fig. 1) show good reproducibility and the utility of this technique for both optically-thick and thin plasmas.

Although it is not our purpose to develop a technique for plasma diagnostics, the electron density will be estimated by several procedures in order to compare the experimental results with computer

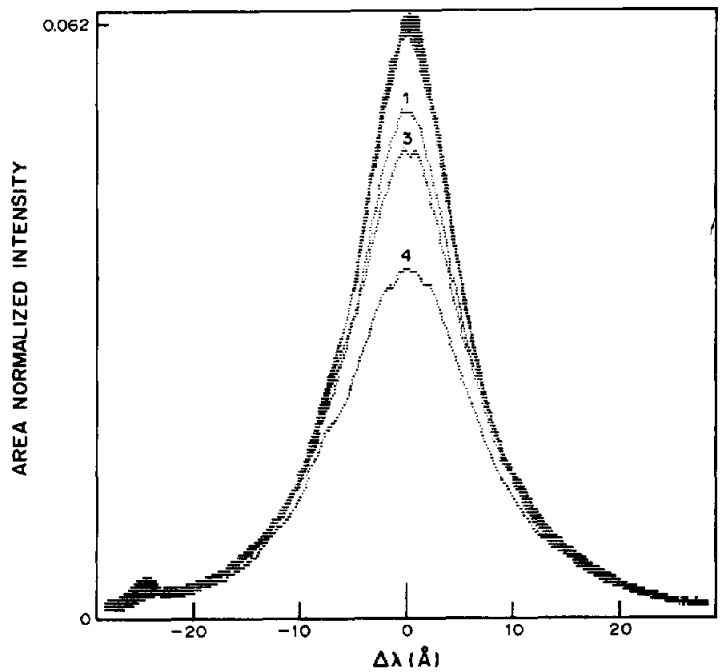

Fig. 1. Three experimental profiles are shown for different self-absorption conditions (experiments 1, 3 and 4), as well as the corrected profile with error bounds. The area under the curve has been normalized to unity.

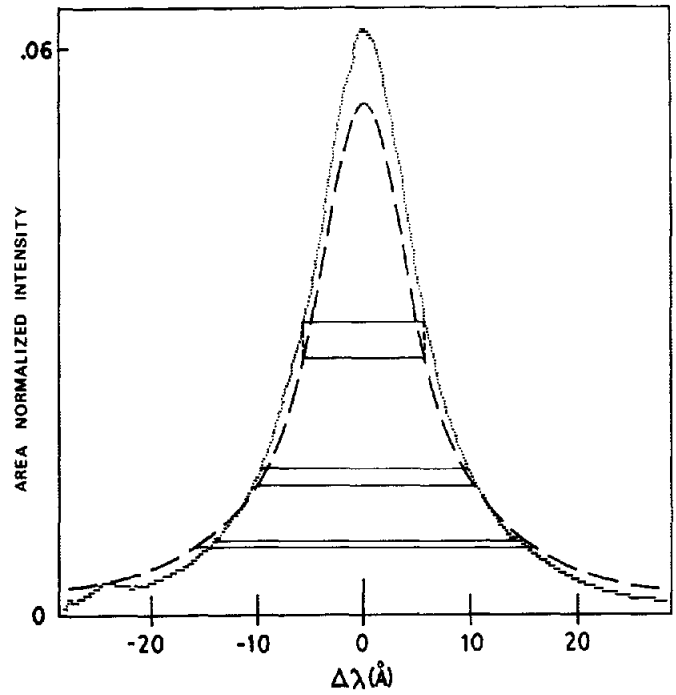

Fig. 2. Comparison of the averaged reconstructed profile (· · ·) with the simulated profile[13] (– – –) that has practically the same full half-width. The simulated profile corresponds to an electron density of $N_e = 1.28 \times 10^{17}$ cm^{-3}. The experimental profile has been smoothed.

simulations. A temperature of 15,000 K was deduced from the relative intensity of the 430.0 nm ArI line to that of the 480.6 nm ArII line. The Doppler width at this temperature is approx. 0.57 Å.

Ehrich and Kelleher[8] summarize data on full half-widths vs electron densities, done by several authors: Ehrich and Kelleher, Ehrich and Kusch, and Wiese (this author's measurements were done

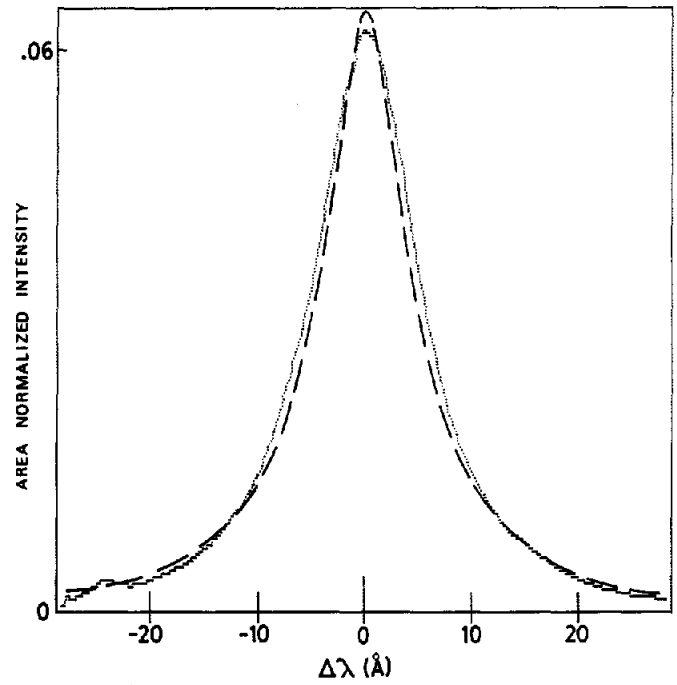

Fig. 3. Comparison of the averaged reconstructed profile (· · ·) with the simulated profile[13] (– – –) that has the lowest deviation from the experimental profile in a spectral range within 25 Å of the line centre. The simulated profile has an electron density of $N_e = 0.96 \times 10^{17}$ cm^{-3}.

in a plasma very similar to ours). From these data, we obtain the relation

$$\log(N_e) = 15.31 + 1.724 \times \log(\Delta\lambda_{1/2}) \quad (3)$$

for our temperature range. The electron density N_e is measured in cm^{-3} and the full half-width $\Delta\lambda_{1/2}$ in Å. Using our measured value of $\Delta\lambda_{1/2}$ for the self-absorbed Balmer-alpha profile, Eq. (3) yields an electron density $N_e = 1.36 \times 10^{17}\ cm^{-3}$ for our plasma.

We next compare this result with recent calculations based on simulation techniques, in which both electron and ion fields are jointly generated[13] so that time-ordering effects naturally arise. In this technique, the relative motion of the radiating ion-perturber is aproximately reproduced by using the μ-ion model; our plasma corresponds to a reduced mass $\mu = 0.975$. The simulated profile that has practically the same full half-width as the experimental profile, corrected for self-absorption, has an electron density $N_e = 1.28 \times 10^{17}\ cm^{-3}$ for a temperature of $\sim 15{,}000$ K. There is therefore reasonable agreement with the result obtained before. The simulated and corrected profiles can be seen in Fig. 2.; the experimental profile has been previously smoothed. Figure 2 shows that the central zone is lower in the simulated than in the experimental profile, although both profiles have similar widths for fractions of the total heights about 1/4. The simulated profile becomes progressively wider than the experimental profile as we move away from the line centre. On the other hand, the simulated profile with smaller deviation from the experimental profile, within a spectral range of 25 Å around the line centre, corresponds to an electron density $N_e = 0.96 \times 10^{17}\ cm^{-3}$. The full half-width of the simulated profile is 1 Å less than the experimental profile. Their representations are shown in Fig. 3.

Acknowledgements—The authors thank M. A. Gigosos and V. Cardeñoso for permission to use unpublished results of their model calculations for the Balmer-alpha line. This work was financially supported by the Spanish "Comisión Asesora para la Investigación en Ciencia y Tecnología" (CAICYT) under Grant No. 3121/83.

REFERENCES

1. M. A. Gigosos and V. Cardeñoso, *J. Phys. B: Atom. Molec. Phys.* **20,** 6005 (1987).
2. J. Seidel, *Z. Naturf.* **32a,** 1207 (1977).
3. C. R. Vidal, J. Cooper, and E. W. Smith, *Astrophys J. Suppl.* **25,** 37 (1973).
4. P. Kepple and H. Griem, *Phys. Rev.* **173,** 317 (1968).
5. W. L. Wiese, D. E. Kelleher, and V. Helbig, *Phys. Rev.* **A11,** 1854 (1975).
6. W. L. Wiese, D. E. Kelleher, and D. R. Paquette, *Phys. Rev.* **A6,** 1132 (1972).
7. K. Grutzmacher and B. Wende, *Phys. Rev.* **A16,** 243 (1977).
8. H. Ehrich and D. E. Kelleher, *Phys. Rev.* **A21,** 319 (1980).
9. F. Torres, M. A. Gigosos, and S. Mar, *JQSRT* **31,** 265 (1984).
10. D. D. Burgess, G. Kolbe, and C. St. Q. Playford, *Spectral Line Shapes*, p. 119, Wende, Berlin (1981).
11. J. Hernández, F. Torres, S. Mar, and M. A. Gigosos, *JQSRT* **33,** 35 (1985).
12. A. Czernichowski and J. Chapelle, *Acta Phys. Pol.* **A63,** 67 (1983).
13. M. A. Gigosos and V. Cardeñoso, private communication (1988).
14. A. Goly, D. Rakotoarijimy, and S. Weniger, *JQRST* **30,** 417 (1983).